In-pile tensile creep of chemical vapor deposited silicon carbide at 300°C[*]

Takaaki Koyanagi[1†], Kurt Terrani[1], Torill Karlsen[2], Vendi Andersson[2], David Sprouster[3], Lynne Ecker[3], Yutai Katoh[1]

1 Oak Ridge National Laboratory, Oak Ridge, TN 37831 United States

2 OECD Halden Reactor Project, Halden, Norway

3 Brookhaven National Laboratory, Upton, NY 11973 United States

Abstract

Irradiation-induced creep is one of the key material properties considered in designing structural components for nuclear reactors. This paper presents results for in situ irradiation-induced creep of chemical vapor–deposited 3C silicon carbide studied by instrumented irradiation in the Halden reactor in Norway. The specimens examined were irradiated at 300°C and up to 2.5×10^{24} n/m^2 (E >0.1 MeV) under uniaxial tensile stress of <5 or 100 MPa. Irradiation-induced creep strain was defined as the differential time-dependent strain between the two specimens. Based on the dimensional inspections before and after irradiation, an axial primary creep strain of 0.06% was obtained at the end of irradiation. The lattice constant precisely determined from high-energy x-ray diffraction analysis showed a lattice expansion roughly accounting for the primary irradiation creep strain. Analysis of data from this and previous studies indicates that creep strain is significantly dependent on at least one of the experimental conditions, such as loading mode, neutron spectrum/flux, and material grade.

Keywords: SiC, irradiation creep, microstructure, neutron irradiation

† Corresponding author. Materials Science and Technology Division, Oak Ridge National Laboratory, 1 Bethel Valley Road, Oak Ridge, TN, 37831-6140, USA.
E-mail address: koyanagit@ornl.gov (T. Koyanagi).

Introduction

To enhance safety margins during severe accidents for light water reactors (LWRs), the development of materials for accident-tolerant fuel cladding was internationally explored with the ultimate goal of replacing the zirconium (Zr) -based alloy cladding currently used in reactors [1]. Silicon carbide (SiC) fiber–reinforced SiC matrix (SiC/SiC) composites possess exceptional oxidation resistance in high-temperature steam environments [2], a relevant condition of loss-of-coolant or beyond-design-basis accidents, and therefore are leading candidates for use as accident-tolerant fuel cladding materials [3–5]. In addition, SiC/SiC composites are anticipated to provide other benefits compared with Zr alloys: unparalleled high-temperature strength [6], smaller neutron absorption cross sections [7], general chemical inertness [8], excellent irradiation resistance of their mechanical properties [9], and lack of progressive irradiation growth [10].

For cladding applications, dimensional evolution—characterized by the amount of swelling and irradiation-induced creep—is of critical importance. For example, the gap between the fuel pellets and the cladding must be well controlled for SiC/SiC composites to manage the stress concentration due to mechanical interaction between the two; diametral swelling of the cladding is the primary controlling factor [11]. In addition, temperature-dependent and neutron dose–dependent swelling of SiC [12] is expected to cause axial bowing if it remains unconstrained and to cause significant internal strain, which may be beyond the matrix cracking stress, in the presence of temperature and/or dose gradients within the cladding [11,13]. Some irradiation-induced creep is desirable in LWR cladding to alleviate stress due to pellet/cladding mechanical interaction [1]. The purpose of this study was to quantify with high accuracy the swelling and irradiation-induced creep behavior of high-purity, highly crystalline SiC at LWR-relevant temperatures. These data are critical to inform ongoing fuel system design and performance analysis to enable deployment of accident-tolerant SiC/SiC cladding concepts.

Irradiation-induced creep in SiC is relatively unknown compared with radiation-induced swelling, primarily because of the difficulty of conducting experiments. Previous experiments on SiC have quantified creep during post-irradiation examination using the bend stress relaxation (BSR) technique [14–16]. This method is very useful in terms of its applicability to miniature specimens and the ease of using it to apply stress to specimens in an irradiation vehicle. It enables the evaluation of irradiation-induced creep of SiC with various forms under a wide range of irradiation temperature and dose conditions [14–16]. Despite these advantages, however, analysis of the results is difficult: the stress state during the test is complex, particularly if the creep strain is not proportional to the magnitude of the applied stress [17]. In such cases, determining the creep strain is challenging. In addition, it is difficult to evaluate the effect of the applied stress level on the creep strain because the applied stress is not constant for BSR tests. Therefore, the BSR experiments did not provide accurate creep rates. These results did reveal the transient and post-transient creep behavior of SiC materials at temperatures under which thermal creep is negligible, and they demonstrated the effects of the material grade on creep resistance [14–16].

To acquire more reliable creep data and better understanding of creep in SiC under irradiation, this study conducted instrumented in-pile tensile creep testing of high-purity chemical vapor–deposited (CVD) 3C SiC. The advantage of this testing is that it provided a continuous record of specimen deformation under a constant applied load, which was previously not available from our past BSR experiments. To the best of our knowledge, this in-pile creep measurement of SiC is the first of its kind, although in situ ion-

irradiation creep tests have been conducted [18]. Post-irradiation high-energy x-ray diffraction (XRD) and electron microscopy analysis was also performed to elucidate the underlying creep mechanism.

Experiment

An irradiation creep experiment was conducted using two SiC tensile specimens at a constant temperature of 300°C under an inert gas atmosphere in the Halden reactor (Norway). The Halden reactor is a heavy water boiling system with a highly thermal spectrum. At the precise location of the irradiation vehicle (IFA-744 rig), the total neutron flux was 1.20×10^{18} n/m^2-s (9.43×10^{16} n/m^2-s [E >0.1 MeV] and 3.50×10^{16} n/m^2-s [E >1 MeV]). Although thermal neutrons are dominant in the Halden reactor, our calculations considering the neutron energy spectrum [19] and displacement per atom (dpa) cross section from reference [20] showed that displacement damage was mainly caused by fast neutrons (E >0.1 MeV). It is assumed that 1 dpa is equivalent to 1×10^{25} n/m^2 (E >0.1 MeV) so that the results obtained from this study can be compared with those from previous studies. In-pile instrumentation and control systems were used to apply stress and record specimen displacement continuously. The specimen temperature was monitored during irradiation using multiple thermocouples along the length of each specimen. The temperature was controlled by a flow of inert gas in the annular regions of the irradiation vehicle. The stress on the creep specimen was controlled by direct gas pressure inside the bellows attached to one end of the creep specimen. The specimen deformation was measured directly using a calibrated linear variable differential transformer (LVDT) that was in contact with the other end of the specimen. More details of the instrumented irradiation vehicle and in-pile creep test are available in ref. [19].

Throughout the experiment, the total strain of the material under uniaxial tensile stress and the in-pile conditions was measured. This quantity is a sum of strains (ε_{total}) due to elastic strain (ε_{ES}), thermal expansion (ε_{TE}), linear swelling (ε_{LS}), thermal creep (ε_{TC}), and irradiation creep (ε_{IC}), as shown in Eq. (1).

$$\varepsilon_{total} = \varepsilon_{ES} + \varepsilon_{TE} + \varepsilon_{LS} + \varepsilon_{TC} + \varepsilon_{IC} \qquad (1)$$

At a constant load and temperature, ε_{ES} and ε_{TE} are constant, but ε_{LS}, ε_{TC}, and ε_{IC} are time-dependent and need to be distinguished. Note that the coefficient of thermal expansion of SiC was reported to be insensitive to irradiation defects [21]. A value of nil (0) is assigned to ε_{TC} at 300°C, since thermal creep operates at temperatures > ~1000°C in SiC [22]. To separate ε_{LS} and ε_{IC}, this study conducted the creep tests with two different loading conditions: 100 MPa and a minimal stress level of <5 MPa. If the minimal stress is applied, ε_{IC} is considered nil, and ε_{LS} can be obtained. Therefore, ε_{IC} can be given by

$$\varepsilon_{IC} = \varepsilon_{100MPa} - \varepsilon_{<5MPa} - \varepsilon_{ES100MPa}, \qquad (2)$$

where ε_{100MPa} and $\varepsilon_{<5MPa}$ are the total strains of the specimens with 100 MPa applied and the minimal stress during irradiation, respectively. $\varepsilon_{ES100MPa}$ is the elastic strain under a tensile stress of 100 MPa. Note that $\varepsilon_{ES100MPa}$ is nil for out-of-pile experiments. To avoid any errors due to a possible mismatch between

zero strain reference points, only the time dependence of the strain was taken into account in the present study. Therefore, the difference in elastic strain between the two specimens was inconsequential during in-pile measurement.

The two tensile specimens were machined from high-purity CVD 3C SiC. The CVD variant (purity >99.999%) was purchased from Dow Chemical Co. (Marlborough, MA). The elastic modulus and average grain size of the material were 466 GPa and 5 µm, respectively, according to the material data sheet provided by the vendor. The grain texture of this material was reported to be moderate [15]. The specimens were machined so that the uniaxial loading direction was perpendicular to the CVD growth direction. The specimens were not annealed after the CVD processing step. The specimen appearance is shown in Fig. 1a. The total length of the specimen was 106 mm, and the gauge section had a length of 50 mm and a diameter of 2.6 mm. Thirteen fiducial marks were etched on the gauge section of each specimen (Fig. 1a, b). More details for the in-pile creep test can be found elsewhere [19].

The distances between the marks before and after irradiation were measured accurately to provide the basis for verification or calibration of in-pile strain data during the post-irradiation examination. Measurements were conducted using a KEYENCE VHX-1000 digital microscope via an XY coordinate value of a stage with a movement accuracy of less than 1 µm. The same equipment was used for both nonirradiated and irradiated specimens. The microscope was operated at a high magnification of ×3000–×5000 so that the center of the mark was precisely determined for distance measurement. The nominal spacing between marks was 5 mm in the unirradiated sample. The practical error of the measurement due to defining the center of the mark (Fig. 1b) was ~1 µm, which is less than or equal to an ~0.04% error in the irradiation-induced strain measurement. Both irradiated specimens were broken upon extraction from the radiation vehicle. As the result, only total distances of 9 marks and 5 marks on the undamaged gauge portions could be measured for the specimens irradiated with applied stresses of <5 and 100 MPa, respectively, although a 12-mark distance was available before irradiation. In spite of the damage to the specimen for the <5 MPa load test, it was possible to compare the mark distance at the same position before and after irradiation. However, that was not possible in the case of the specimen with an applied stress of 100 MPa, so the average value of the mark distance was used to evaluate the in-pile deformation.

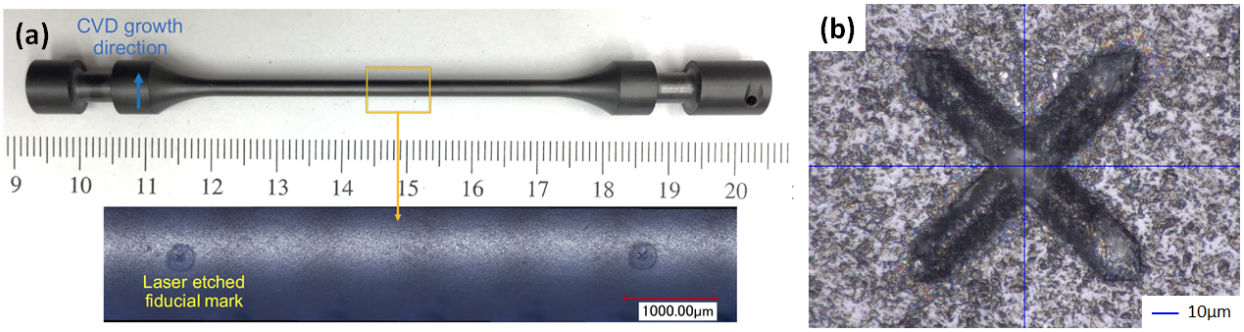

Fig. 1 (a) Appearance of unirradiated tensile specimen made of monolithic CVD SiC and (b) laser-engraved mark observed following neutron irradiation. The cross-point of the blue lines in image (b) indicates the center of the engraved mark used to measure the mark distance.

Post-irradiation examination also included high-energy XRD experiments at the Powder X-ray Diffraction beamline of the National Synchrotron Light Source-II at Brookhaven National Laboratory [23,24]. XRD measurements were performed in transmission mode with an amorphous silicon-based flat panel detector (PerkinElmer) mounted orthogonal to and centered on the beam path. The sample-to-detector distances and tilts of the detector relative to the beam were refined using an LaB_6 powder standard (NIST standard 660c). The wavelength of the incident x-rays was 0.2370 Å (52.31 keV). The sample-to-detector distance was 1351.94 mm. The gauge section of the irradiated tensile bars was machined into disc specimens of 2.6 mm diameter and 1–1.5 mm thickness. Five and seven individual irradiated specimens were evaluated for applied stresses of 100 and <5 MPa, respectively. Three pristine unirradiated specimens were also evaluated. The beam direction was parallel to the specimen thickness direction. The specimens were wrapped with Kapton film to fix them onto a dedicated holder and to limit radiological exposure. Samples were continuously rotated during acquisition to improve the powder averaging. XRD images were collected with 0.5 sec acquisition times. Each diffraction pattern consisted of the average of 100 individual exposures. Noticeable artifacts in the images (like the beam stop or dead pixels) were masked. The two-dimensional detector images were radially integrated to obtain one-dimensional powder diffraction patterns. All XRD patterns were background corrected by subtracting the Kapton/air scattering component. The corrected XRD patterns were Rietveld-refined using Bruker TOPAS software; lattice constant, coherent grain size, and anisotropic micro-strain were refined within the Rietveld cycles. The peak profiles were modeled by a modified pseudo-Voigt function. Peak broadening arising from any instrument contribution was quantified by fitting the pattern of the LaB_6 powder so that the anisotropic micro-strains and coherent grain sizes of the specimens were obtained from the Rietveld refinement.

Transmission electron microscopy (TEM) using a JEOL JEM2100F operating at 200 kV was employed to observe the microstructure of the specimens. TEM foils were taken from the gauge section of the tensile bar using a focused ion beam (a FEI Quanta Dual Beam) operating at 30 kV for rough milling and at 2–5 kV for final polishing. The foil thickness direction was perpendicular to the tensile stress direction. A weak-beam dark-field (WBDF) technique with a g/3–4g condition was used to observe processing and radiation defects. The foil thickness was evaluated by means of an electron-energy-loss spectroscopy log-ratio technique.

Results

Figure 2 shows recorded in-pile measurements of the displacement of the SiC specimens. The targeted temperature and applied stress levels were achieved during most of the period of the in-pile experiment. In addition, the fast neutron flux was kept at ~3×10^{16} n/m^2-s [19]. The record of the specimen displacement shows a clear and significant departure in strain between the two samples upon the application of 100 MPa or <5 MPa of stress. This time-dependent difference in the specimen displacement is explained by irradiation-induced creep, based on Eq. (2). The total displacement at the end of irradiation to 0.25 dpa was 610 and 390 μm for the SiC specimens with applied stresses of 100 MPa and <5 MPa, respectively. Figure 2 also shows the “shifted” displacement curve of the specimen with applied stress of 100 MPa to compare the deformation behavior with and without applied stress. Similar deformation behavior was found regardless of the applied stress in the case of neutron fluence beyond ~1.5×10^{24} n/m^2 (E >0.1 MeV), indicating that the applied stress had only a limited effect on the length change of the specimen at such relatively high neutron doses.

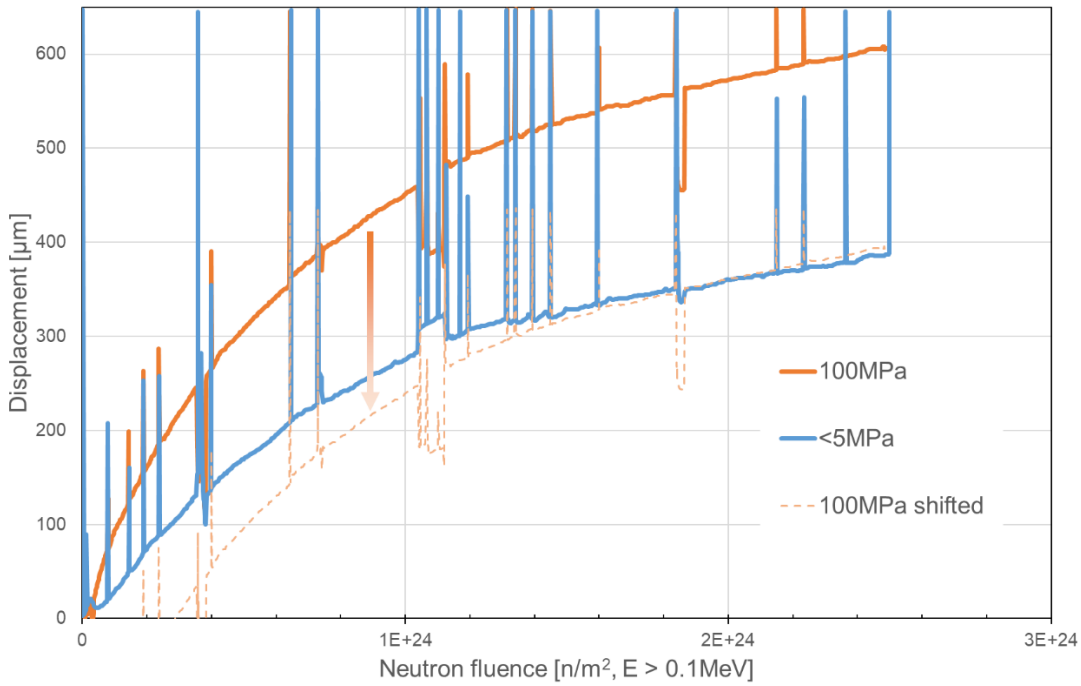

Fig. 2 Recorded specimen displacement during in-pile creep test of CVD SiC. The figure also shows the "shifted" displacement curve of the specimen with applied stress of 100 MPa to compare deformation behavior with and without applied stress.

The measurement results for the fiduciary mark spacing conducted before and after irradiation are shown in Table 1, together with the in-pile displacements of the specimens. The changes in fiduciary mark spacing showed swelling of 0.42 % and creep strain of 0.06 %. Note that the creep strain was obtained based on Eq. (2). It was found that the in-pile strain measurements for the specimens subjected to <5 MPa stress reasonably matched the measured changes in fiduciary mark spacing. However, the creep strain of 0.44% derived from the in-pile displacement and Eq. (2) for the specimen loaded to 100 MPa was about one order of magnitude larger than that determined from measurement of the fiduciary mark spacing.

Table 1 Summary of results of in-pile strain measurement, post-irradiation strain measurement, and XRD analysis. Parentheses indicate one standard deviation unless otherwise indicated. Definition of irradiation creep strain is described by Eq. (2). Note that discrepancy among in-pile and out-of-pile creep strain is due to uncertainty of the in-pile strain measurement, as explained in the manuscript.

Test condition	Applied stress during irradiation	XRD analysis			Swelling [%]	Irradiation creep strain [%]
		Lattice constant [Å]	Coherent grain size [nm]	Anisotropic micro-strain		
Unirradiated	Not available (NA)	4.361537 (0.000581)	139.9 (56.0)	0.0353 (0.0035)	NA	NA
Irradiated at 300°C to 0.25dpa	<5 MPa	4.380248 (0.000529)	110.7 (6.2)	0.0428 (0.0089)	In-pile: 0.37 Engraved mark: 0.42 (0.04*) Lattice (XRD): 0.429 (0.012)	NA
	100 MPa	4.381455 (0.000601)	99.1 (16.1)	0.0420 (0.0122)	NA	In-pile: 0.44 Engraved mark: 0.06 (0.04*) Lattice (XRD): 0.028 (0.014)

*Uncertainty of measurement using optical microscope

Figure 3 shows averaged XRD patterns for each test condition. All the specimens exhibit a β-SiC phase with an F-43m crystal structure. A small shoulder peak at ~5.1 degrees is also a common feature, which indicates the presence of stacking faults [25]. The XRD patterns show that neutron irradiation results in a clear shift of the peaks to lower two-theta angles. In addition, the applied stress during irradiation caused a further peak shift to lower angles, as shown in the enlarged figure, although the peak shift is small. These peak shifts to lower two-theta angles are indications of lattice expansion. The lattice constant, coherent grain size, and anisotropic micro-strain determined by Rietveld refinement are summarized in Table 1. Irradiation-induced lattice expansion was 0.43% when the minimal stress was applied. According to Eq. (2), the irradiation creep strain due to lattice expansion was 0.028±0.014%, which is the difference of lattice strain with and without 100 MPa tensile stress. This value was of the same order of magnitude as the macroscopic creep strain of 0.06% obtained from the measurements of the fiduciary marks. The effects of irradiation on the coherent grain size and micro-strain were limited regardless of the applied stress level.

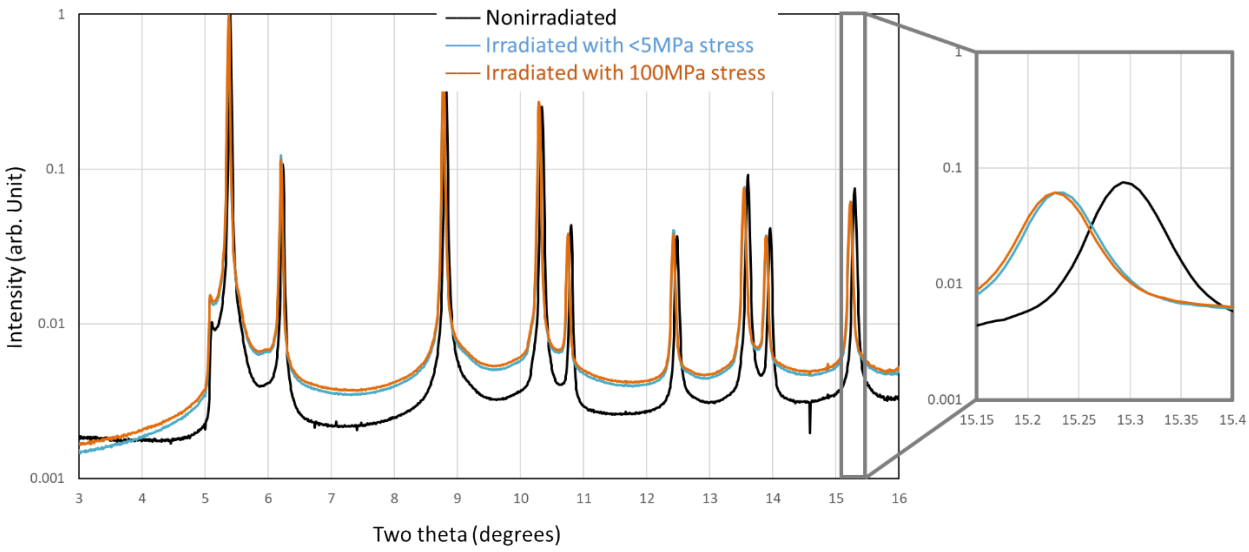

Fig. 3 Averaged XRD patterns of CVD SiC unirradiated and irradiated at 300℃ to 0.25 dpa with applied stress of <5 and 100 MPa.

The grain size of the reference specimen was a few microns, based on TEM observations, as shown in Fig. 4a, which was consistent with the nominal grain size provided by the vendor. There was no notable change in grain size and no indication of grain boundary sliding (such as voids at grain boundaries) following irradiation at a tensile stress of 100 MPa, as shown in Fig. 4b. Figures 4c–e are WBDF TEM micrographs of the pristine and irradiated SiC. All the images were taken at a $\boldsymbol{g}$ = <220> condition. The unirradiated material had stacking faults as processing defects, which was consistent with the shoulder peak at ~5.1 degrees in the XRD pattern. There was no notable change in the appearance of the stacking faults due to irradiation. In contrast, irradiation introduced small defect clusters in the WBDF micrographs following irradiation, which were not detected in the pristine specimen. Regardless of the applied stress level, the defect diameter and density were 1–2 nm and ~1×10^{23} m^{-3}, respectively. The habit plane and Burgers vector of the defects could not be identified because of their small size.

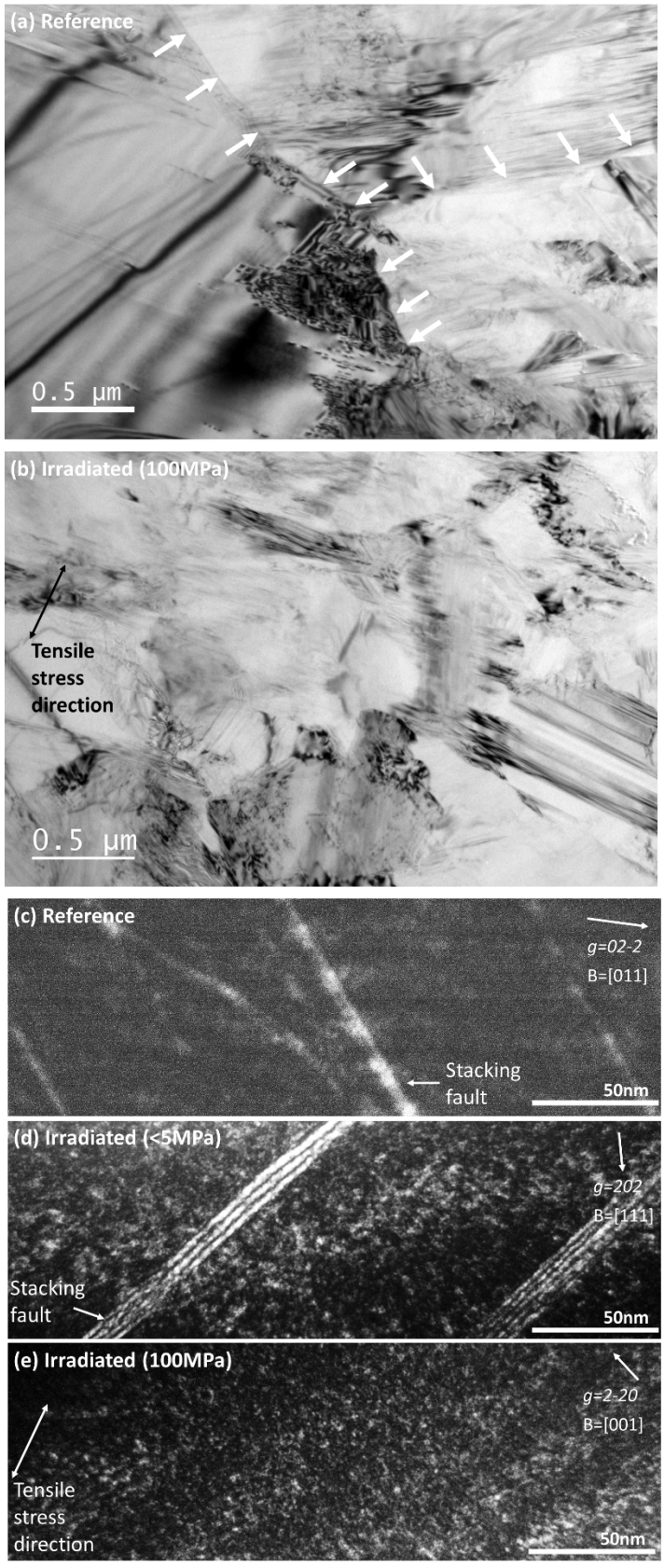
(a) Reference
0.5 μm
(b) Irradiated (100MPa)
Tensile stress direction
0.5 μm
(c) Reference
g=02-2
B=[011]
Stacking fault
50nm
(d) Irradiated (<5MPa)
g=202
B=[111]
Stacking fault
50nm
(e) Irradiated (100MPa)
g=2-20
B=[001]
Tensile stress direction
50nm

Fig. 4 Bright-field TEM micrographs of CVD SiC: (a) unirradiated and (b) irradiated at 300℃ to 0.25 dpa under 100 MPa tensile stress. Weak-beam dark-field micrographs of CVD SiC: (c) unirradiated and irradiated under (d) <5 MPa and (e) 100 MPa stress. Grain boundaries are indicated by arrows in Fig. (a). The beam direction and $\boldsymbol{g}$ vector used for the dark-field imaging are indicated in Figs (c)–(e).

Discussion

It was found that, for the same specimen, irradiation creep strains measured by the in-pile instrumentation and out-of-pile dimensional measurements of the fiducial mark spacing showed considerable discrepancy in the case of the applied 100 MPa tensile stress (Table 1), which was far beyond the measurement uncertainty. There was potential for the deformation of the test fixture and loading devices due to irradiation to cause uncertainties in the in-pile strain measurement, although load measurement was not affected by the component deformation because the load was controlled by gas pressure. It is likely that the additional specimen displacement was caused by stress concentration at the specimen grip and/or loading section, since strain measurement with a LVDT is reliable. A general specimen grip system cannot avoid stress concentration, which may cause irradiation creep in loading fixtures and consequently cause error in strain measurement. Therefore, an out-of-pile strain measurement is required although this has not always been conducted in previous in-pile creep studies. In addition, the process for adjusting the in-pile data based on out-of-pile data has not been standardized and discussed well.

This section explains the in-pile creep data considering the additional deformation of the loading system. Both CVD SiC specimens, with and without applied stress, showed very similar changes in displacement against the neutron fluence beyond ~1.5×10^{24} n/m^2 (E >0.1 MeV); these were clearly found when the displacement curve of the specimen with 100 MPa stress was shifted to lower values for comparison purposes, as shown in Fig. 2. This result indicates that the applied stress (irradiation creep strain) had a limited effect on the change in the specimen length at a relatively high neutron dose. This explanation is supported by the current understanding of irradiation creep in SiC: insignificant irradiation creep at such a high neutron dose (beyond ~0.15 dpa in this case) occurred because this dose level corresponds to the end of the transient creep regime and the creep rate becomes insignificant beyond this point based on the previous study [16].

In the case of the specimen without applied stress, a successful measurement of the specimen length change without stress (swelling) was demonstrated based on the out-of-pile dimensional evaluation. Figure 5a compares dose-dependent swelling of CVD SiC neutron irradiated in the Halden reactor and in the High Flux Isotope Reactor (HFIR) at Oak Ridge National Laboratory [26]. The irradiation temperature was 300℃ for both cases, and the same grade of CVD SiC material was used. On the other hand, the neutron spectra and fluxes of these reactors were different, resulting in approximately a two-orders-of-magnitude difference in the displacement damage rate: 9.43×10^{-9} dpa/s for the Halden reactor and ~1×10^{-6} dpa/s for the HFIR. Length change of the CVD SiC irradiated in the Halden reactor was found to be smaller than the swelling after irradiation in HFIR by ~0.2 % at 0.1 dpa. This difference was beyond the background noise of the in-pile displacement measurement (< 0.01 %). This finding showed that a different irradiation environment (likely a different neutron spectrum or flux) affected the swelling behavior. Considering the ignorable mobility of vacancies at 300℃ due to the high migration energies [27], annihilation and

clustering of self-interstitial atoms played an important role in the dose-rate effect on swelling. Even though the dose rate was different, both the specimens irradiated in the Halden reactor and those irradiated in HFIR exhibited similar microstructural features with high-density defect clusters, as shown in Fig. 4 and as reported in [28]. The similarities indicate a similar swelling mechanism, so-called point-defect swelling [12]. The swelling mechanism is discussed along with the creep mechanism later.

Irradiation creep behavior by comparison with results from this and previous studies [15] is discussed here; Figure 5b shows the irradiation creep compliance, normalized creep strain with respect to applied stress and neutron dose, to indicate creep rate and to compare the creep behavior of different CVD SiC materials under different radiation conditions. A linear normalization was employed for the stress dependence of the creep strain, according to a previous study [15,29]. The creep strain in the present study was obtained based on out-of-pile measurement of tensile creep specimens, whereas previous work used BSR creep specimens. An average applied bend stress during irradiation was within 64–200 MPa. In previous studies, irradiation was conducted in HFIR or the Japan Materials Testing Reactor (JMTR) with a typical damage rate of ~1×10^{-6} dpa/s and ~1×10^{-8} dpa/s, respectively, with an equivalence of 1 dpa = 1×10^{25} n/m^2 (E > 0.1 MeV). In addition, the materials tested varied; they included Dow Chemical (previously Rohm & Hass) polycrystalline 3C SiC with and without heat treatment, Coorstek polycrystalline 3C SiC with heat treatment, and Cree 4H single-crystal SiC. The heat treatment was conducted at 1900°C for 1 h under argon and was expected to modify the grain size and concentration of pre-existing defects, such as stacking faults [30]. The irradiation temperatures ranged from 300 to 600°C, where point defects and their clusters contribute to the dimensional stability of SiC [12].

Despite the use of different materials and irradiation conditions, the measured creep compliances were within the same order of magnitude at the same displacement damage for the BSR tests, as shown in Fig. 5b. This indicates that the BSR transient irradiation creep of SiC is insensitive to the initial material microstructure, damage rate, and irradiation temperature at such intermediate temperatures. In contrast, these differences in experimental conditions caused a more than one order of magnitude higher creep strain under tensile creep than under BSR creep. This result indicates a strong sensitivity of the loading mode to irradiation creep of SiC, considering the lower sensitivity of the BSR creep compliance to different experimental conditions. However, the effect of the loading mode on the creep behavior still needs to be confirmed using the same material irradiated under the same conditions. At the least, it can be concluded that at least one of the following experimental parameters had a significant effect on irradiation creep: loading condition (tensile vs. bend relaxation), displacement damage rate, and initial material microstructure, based on the analysis of creep compliance.

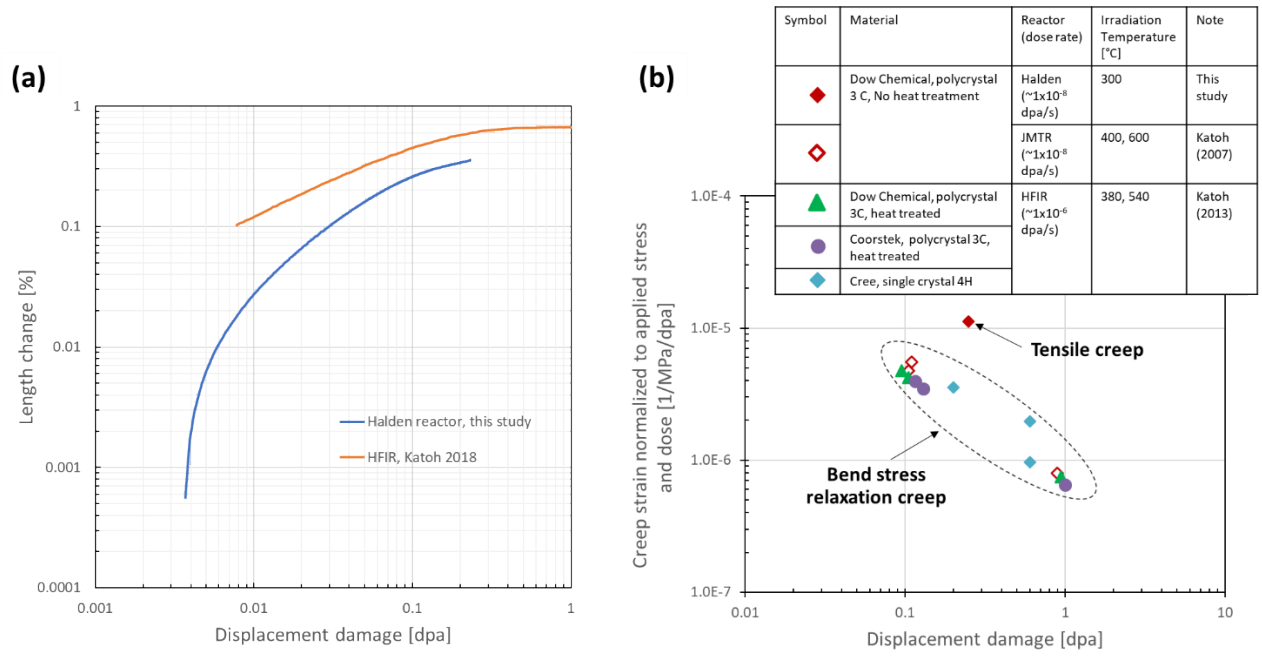

Fig. 5 Displacement damage dependent (a) linear swelling and (b) irradiation creep compliance of CVD SiC. The data from previous studies [15,26] are also plotted. Note that data for the same and different grades of CVD SiC are presented in image (a) and (b), respectively.

Regarding the underlying mechanism of irradiation creep of SiC up to 0.25 dpa where transient creep is dominant [15], It was demonstrated that the lattice strain was of the same order of magnitude as the macroscopic creep strain shown in Table 1. In addition, the XRD analysis found that the macroscopic swelling and lattice expansion were comparable. Therefore, lattice expansion effectively contributed to the dimensional stability of the CVD SiC. It is known that the magnitude of swelling of SiC is almost identical to the magnitude of the lattice expansion under irradiation at intermediate temperatures (300–800°C) to a relatively low neutron dose (<~10 dpa) [31,32]. Therefore, this study provides additional confirmation of the relationship between swelling and lattice expansion. Lattice expansion is caused by atomistic defects, including the small defect clusters observed in TEM and point defects [12]. Moreover, the increment of lattice expansion due to applied stress is an indication of a creep mechanism related to lattice expansion. A previous study correlated radiation creep strain with swelling and provided a mechanistic creep model assuming anisotropic swelling due to applied stress [15]. A strong relationship between swelling and irradiation creep in a transient regime up to ~1 dpa is the current understanding regarding the creep mechanism [15,33].

Although the results indicate an irradiation creep mechanism related to lattice strain, it is still not clear what kind of radiation defect causes lattice extension. The TEM observations could not identify any effect of applied stress on the microstructural evolution, suggesting that only atomistic defects were causing changes in the lattice constant. Similarly, the coherent grain size and anisotropic strain obtained from the XRD peak broadening analysis did not reveal any effect of applied stress. It was reported that decreasing coherent grain size and increasing anisotropic strain are indications of the growth of dislocation loops in SiC [31]. The insensitivity of the coherent grain size and the anisotropic strain to applied stress during

irradiation indicated that a 100 MPa stress had a limited effect on the microstructural evolution. It is possible that both the TEM WBDF imaging and the XRD peak broadening were insensitive to the defects that caused irradiation creep. It is also possible that the anisotropy of defect evolution under applied stress contributed to creep strain (e.g., more defects formed along the tensile stress direction) [34] so that the microstructures with and without applied stress appeared to be similar.

Previously proposed creep mechanisms [35] that might explain the observed lattice expansion due to applied stress during irradiation include stress-induced preferential nucleation of loops (SIPN) [34] and stress-induced preferential absorption (SIPA) of self-interstitial atoms [36]. SIPN occurs when the application of external stress enhances the probability of interstitial loops on planes under tensile stress. Such preferential loops cause increases in length in the direction of the tensile stress, which contribute to irradiation creep strain. The increment of lattice expansion due to the applied tensile stress revealed by the XRD analysis was consistent with this mechanism because the formation of intestinal-type defects contributes to lattice expansion. Since the size of the irradiation defect clusters was quite small (1–2 nm) based on the TEM analysis, preferential nucleation of interstitial clusters, in addition to intestinal loops, was thought to contribute to creep strain. SIPA has been proposed as a mechanism of steady state irradiation creep associated with preferential growth of interstitial loops due to the transfer of interstitial atoms from planes parallel to the applied stress, to planes perpendicular to the applied stress. The growth of loops along the tensile stress direction contributes to macroscopic strain. This mechanism is also consistent with the XRD results for the enhanced lattice expansion under in-pile tensile stress. The SIPA mechanism may operate at relatively high displacement damage, as it requires the growth of interstitial loops and clusters.

Irradiation creep strain as the result of the preferential nucleation/growth of interstitial loops can be expressed as follows [35]:

$$\varepsilon = 2/3 f \pi r_L^2 b N_L \qquad (3)$$

where f is the excess fraction of intestinal loops on the plane perpendicular to tensile stress, r is the loop radius, b is the Burgers vector, and N_L is the total loop concentration. Equation (3) assumes the presence of only three types of loops for simplicity: loops on two types of planes parallel to stress axis and on one plane perpendicular to the stress direction [35]. Assuming an extreme case of $f = 1$ in which all the defect clusters/loops are formed in the preferential orientation due to the applied stress, one can calculate creep strain with input parameters of r_L: 1 nm, b: a/3<111>, and N_L: 1×10^{23} m^{-3}. The loop size and density are based on the TEM observation conducted. The Burgers vector for a Frank faulted loop is assumed according to previous observations [28], although this study could not identify the nature of the defects. The calculation showed irradiation creep strain of ~0.005%, which was only ~9% of the macroscopic creep strain obtained. Because of the extreme assumption, a smaller contribution of the defects observed in TEM to the bulk creep strain was expected. This result implies that the conventional TEM observation could not capture the majority of the radiation defect clusters affecting irradiation creep because of the image resolution. The implications of such “invisible” defect clusters in TEM have also been reported [37]. Future work will involve advanced characterization of the atomistic defects in irradiated SiC. In addition, as discussed earlier, a comparison of irradiation creep behavior among this and previous studies (Fig. 5b)

shows a potential impact of the microstructure of the starting material on radiation creep. Therefore, it is necessary to investigate the effects of pre-existing defects, such as grain boundaries and stacking faults, on irradiation creep in future studies.

Conclusion

"This study explores the transient irradiation creep behavior of a high-purity CVD 3C SiC monolith under constant uniaxial tensile loading conditions. Findings are summarized as follows.

- Swelling behavior was clearly different between in the Halden reactor and in HFIR, with different neutron spectra, although the magnitude of the difference was not significant.
- According to the dimensions measured before and after irradiation, a creep strain of 0.06% was obtained for irradiation at 300℃ to 2.5×10^{24} n/m^2 (E >0.1 MeV) under a uniaxial tensile stress of 100 MPa. This macroscopic creep strain had same order of magnitude of creep strain obtained from the lattice constant of irradiated SiC.
- The tensile radiation creep strain value found in this study was more than one order of magnitude larger than the reported strain obtained by bend stress relaxation experiments under various material and irradiation conditions. The analysis suggests that creep strain is significantly dependent on at least one of the experimental conditions—loading mode, neutron spectrum/flux, and material grade.
- TEM observation suggested that atomistic radiation defects caused the lattice expansion regardless of the presence of applied stress during irradiation.
- In future work, it is necessary to investigate the effects of loading mode, neutron flux, and material microstructure on irradiation creep and to understand the effect of atomistic defect formation on deformation, as the magnitude of the irradiation creep for CVD SiC for LWR clad applications is still inconclusive.

Acknowledgments

This study was supported by the US Department of Energy (DOE), Office of Nuclear Energy, for the Advanced Fuels Campaign of the Nuclear Technology R&D program under contact DE-AC05-00OR22725 with Oak Ridge National Laboratory (ORNL), managed by UT Battelle, LLC. The high-energy XRD and TEM experiments were supported by the Office of Nuclear Energy under DOE Idaho Operations Office Contract DE-AC07- 051D14517 as part of a Nuclear Science User Facilities experiment. This research used the x-ray powder diffraction beamline at the National Synchrotron Light Source-II, a DOE Office of Science User Facility operated for the DOE Office of Science by Brookhaven National Laboratory under Contract No. DE-SC0012704. Anne Campbell and Timothy Burchell at ORNL provided valuable comments on the manuscript.

The raw/processed data required to reproduce these findings cannot be shared at this time because of technical or time limitations.

References

[1] K.A. Terrani, Accident tolerant fuel cladding development: Promise, status, and challenges, J. Nucl. Mater. 501 (2018) 13–30. doi:10.1016/j.jnucmat.2017.12.043.

[2] K.A. Terrani, B.A. Pint, C.M. Parish, C.M. Silva, L.L. Snead, Y. Katoh, Silicon carbide oxidation in steam up to 2 MPa, J. Am. Ceram. Soc. 97 (2014) 2331–2352. doi:10.1111/jace.13094.

[3] C.P. Deck, G.M. Jacobsen, J. Sheeder, O. Gutierrez, J. Zhang, J. Stone, H.E. Khalifa, C.A. Back, Characterization of SiC-SiC composites for accident tolerant fuel cladding, J. Nucl. Mater. 466 (2015) 1–15. doi:10.1016/j.jnucmat.2015.08.020.

[4] D. Kim, H.G. Lee, J.Y. Park, W.J. Kim, Fabrication and measurement of hoop strength of SiC triplex tube for nuclear fuel cladding applications, J. Nucl. Mater. 458 (2015) 29–36. doi:10.1016/j.jnucmat.2014.11.117.

[5] C. Sauder, Ceramic Matrix Composites: Nuclear Applications, in: Ceram. Matrix Compos. Mater. Model. Technol., 2014: pp. 609–646. doi:10.1002/9781118832998.ch22.

[6] J. Lamon, Chemical Vapor Infiltrated SiC/SiC Composites (CVI SiC/SiC), in: Handb. Ceram. Compos., Springer US, 2005: pp. 55–76. doi:10.1007/0-387-23986-3_3.

[7] N.M. George, K. Terrani, J. Powers, A. Worrall, I. Maldonado, Neutronic analysis of candidate accident-tolerant cladding concepts in pressurized water reactors, Ann. Nucl. Energy. 75 (2015) 703–712. doi:10.1016/j.anucene.2014.09.005.

[8] J. Braun, C. Guéneau, T. Alpettaz, C. Sauder, E. Brackx, R. Domenger, S. Gossé, F. Balbaud-Célérier, Chemical compatibility between UO2 fuel and SiC cladding for LWRs. Application to ATF (Accident-Tolerant Fuels), J. Nucl. Mater. 487 (2017) 380–395. doi:10.1016/j.jnucmat.2017.02.031.

[9] T. Koyanagi, Y. Katoh, Mechanical properties of SiC composites neutron irradiated under light water reactor relevant temperature and dose conditions, J. Nucl. Mater. 494 (2017) 46–54. doi:10.1016/j.jnucmat.2017.07.007.

[10] T. Koyanagi, T. Nozawa, Y. Katoh, L.L. Snead, Mechanical property degradation of high crystalline SiC fiber–reinforced SiC matrix composite neutron irradiated to ~100 displacements per atom, J. Eur. Ceram. Soc. 38 (2018) 1087–1094. doi:10.1016/J.JEURCERAMSOC.2017.12.026.

[11] G. Singh, R. Sweet, N.R. Brown, B.D. Wirth, Y. Katoh, K. Terrani, Parametric Evaluation of SiC/SiC Composite Cladding with UO2Fuel for LWR Applications: Fuel Rod Interactions and Impact of Nonuniform Power Profile in Fuel Rod, J. Nucl. Mater. 499 (2018) 155–167. doi:10.1016/j.jnucmat.2017.10.059.

[12] L.L. Snead, T. Nozawa, Y. Katoh, T.S. Byun, S. Kondo, D.A. Petti, Handbook of SiC properties for fuel performance modeling, J. Nucl. Mater. 371 (2007) 329–377.

doi:10.1016/j.jnucmat.2007.05.016.

[13] M. Ben-Belgacem, V. Richet, K.A. Terrani, Y. Katoh, L.L. Snead, Thermo-mechanical analysis of LWR SiC/SiC composite cladding, J. Nucl. Mater. 447 (2014) 125–142. doi:10.1016/j.jnucmat.2014.01.006.

[14] R.J. Price, Properties of Silicon Carbide for Nuclear Fuel Particle Coatings, Nucl. Technol. 35 (1977) 320–336. doi:10.13182/NT77-A31892.

[15] Y. Katoh, L.L. Snead, C.M. Parish, T. Hinoki, Observation and possible mechanism of irradiation induced creep in ceramics, J. Nucl. Mater. 434 (2013) 141–151. doi:10.1016/j.jnucmat.2012.11.035.

[16] T. Koyanagi, Y. Katoh, K. Ozawa, K. Shimoda, T. Hinoki, L.L. Snead, Neutron-irradiation creep of silicon carbide materials beyond the initial transient, J. Nucl. Mater. 478 (2016) 97–111. doi:10.1016/j.jnucmat.2016.06.006.

[17] G.N. Morscher, C.A. Lewinsohn, C.E. Bakis, R.E. Tressler, T. Wagner, Comparison of Bend Stress Relaxation and Tensile Creep of CVD SiC Fibers, J. Am. Ceram. Soc. 78 (1995) 3244–3252. doi:10.1111/j.1151-2916.1995.tb07960.x.

[18] A. Jankowiak, C. Grygiel, I. Monnet, Y. Serruys, C. Colin, S. Miro, L. Gelebart, L. Gosmain, J.M. Costantini, Advanced SiC fiber strain behavior during ion beam irradiation, Nucl. Instruments Methods Phys. Res. Sect. B Beam Interact. with Mater. Atoms. 314 (2013) 144–148. doi:10.1016/j.nimb.2013.04.031.

[19] K.A. Terrani, T.M. Karlsen, Y. Yamamoto, Fuel Cycle Research & Development Advanced Fuels Campaign Input Correlations for Irradiation Creep of FeCrAl and SiC Based on In-Pile Halden Test Results, ORNL/TM-20 (2016). https://info.ornl.gov/sites/publications/files/Pub62748.pdf.

[20] H.L. Heinisch, L.R. Greenwood, W.J. Weber, R.E. Williford, Displacement damage in silicon carbide irradiated in fission reactors, J. Nucl. Mater. 327 (2004) 175–181. doi:10.1016/j.jnucmat.2004.02.012.

[21] Y. Katoh, T. Nozawa, C. Shih, K. Ozawa, T. Koyanagi, W. Porter, L.L. Snead, High-dose neutron irradiation of Hi-Nicalon Type S silicon carbide composites. Part 2: Mechanical and physical properties, J. Nucl. Mater. 462 (2015) 450–457. doi:10.1016/j.jnucmat.2014.12.121.

[22] J.A. Dicarlo, Creep of chemically vapour deposited SiC fibres, J. Mater. Sci. 21 (1986) 217–224. doi:10.1007/BF01144723.

[23] X. Shi, S. Ghose, E. Dooryhee, Performance calculations of the X-ray powder diffraction beamline at NSLS-II, J. Synchrotron Radiat. 20 (2013) 234–242. doi:10.1107/S0909049512049175.

[24] D.J. Sprouster, R. Weidner, S.K. Ghose, E. Dooryhee, T.J. Novakowski, T. Stan, P. Wells, N. Almirall, G.R. Odette, L.E. Ecker, Infrastructure development for radioactive materials at the NSLS-II, Nucl. Instruments Methods Phys. Res. Sect. A Accel. Spectrometers, Detect. Assoc. Equip. (2018). doi:10.1016/j.nima.2017.10.053.

[25] V. V. Pujar, J.D. Cawley, Effect of Stacking Faults on the X-ray Diffraction Profiles of β-SiC Powders, J. Am. Ceram. Soc. 78 (1995) 774–782. doi:10.1111/j.1151-2916.1995.tb08246.x.

[26] Y. Katoh, T. Koyanagi, J.L. McDuffee, L.L. Snead, K. Yueh, Dimensional stability and anisotropy of

SiC and SiC-based composites in transition swelling regime, J. Nucl. Mater. 499 (2018) 471–479. doi:10.1016/j.jnucmat.2017.12.009.

[27] M. Bockstedte, A. Mattausch, O. Pankratov, Ab initio study of the migration of intrinsic defects in 3C − SiC, Phys. Rev. B - Condens. Matter Mater. Phys. (2003). doi:10.1103/PhysRevB.68.205201.

[28] Y. Katoh, N. Hashimoto, S. Kondo, L.L. Snead, A. Kohyama, Microstructural development in cubic silicon carbide during irradiation at elevated temperatures, J. Nucl. Mater. 351 (2006) 228–240. doi:10.1016/j.jnucmat.2006.02.007.

[29] Y. Katoh, L.L. Snead, T. Hinoki, S. Kondo, A. Kohyama, Irradiation creep of high purity CVD silicon carbide as estimated by the bend stress relaxation method, J. Nucl. Mater. 367–370 A (2007) 758–763. doi:10.1016/j.jnucmat.2007.03.086.

[30] S. Rohmfeld, M. Hundhausen, L. Ley, Influence of stacking disorder on the Raman spectrum of 3C-SiC, Phys. Status Solidi Basic Res. 215 (1999) 115–119. doi:10.1002/(SICI)1521-3951(199909)215:1<115::AID-PSSB115>3.0.CO;2-3.

[31] D.J. Sprouster, T. Koyanagi, E. Dooryhee, S.K. Ghose, Y. Katoh, L.E. Ecker, Microstructural evolution of neutron irradiated 3C-SiC, Scr. Mater. 137 (2017) 132–136. doi:10.1016/j.scriptamat.2017.02.030.

[32] T. Yano, H. Miyazaki, M. Akiyoshi, T. Iseki, X-ray diffractometry and high-resolution electron microscopy of neutron-irradiated SiC to a fluence of 1.9 x 10(27) n/m(2), J. Nucl. Mater. 253 (1998) 78–86. papers2://publication/uuid/5CDB94C6-D4AF-4E4F-A615-B0877E13DC81.

[33] S. Kondo, T. Koyanagi, T. Hinoki, Irradiation creep of 3C-SiC and microstructural understanding of the underlying mechanisms, J. Nucl. Mater. 448 (2014) 487–496. doi:10.1016/j.jnucmat.2013.09.004.

[34] A.D. Brailsford, R. Bullough, Irradiation creep due to the growth of interstitial loops, Philos. Mag. 27 (1973) 49. doi:10.1080/14786437308228913.

[35] G.S. Was, Fundamentals of radiation materials science: Metals and alloys, second edition, 2016. doi:10.1007/978-1-4939-3438-6.

[36] P.T. Heald, M. V. Speight, Steady-state irradiation creep, Philos. Mag. (1974). doi:10.1080/14786437408226592.

[37] B. Tyburska-Püschel, Y. Zhai, L. He, C. Liu, A. Boulle, P.M. Voyles, I. Szlufarska, K. Sridharan, Size distribution of black spot defects and their contribution to swelling in irradiated SiC, J. Nucl. Mater. (2016). doi:10.1016/j.jnucmat.2016.04.044.